HEFAT2012
9th International Conference on Heat Transfer, Fluid Mechanics and Thermodynamics
16 – 18 July 2012
Malta

SIMULATION MODEL OF A SMALL POWER REFRIGERATION CYCLE DEMONSTRATION UNIT

Martínez-Suárez J.A.[a], Sieres J.[a]*, Martín E.[b]
[a]Área de Máquinas y Motores Térmicos, Escuela de Ingeniería Industrial, Campus Universitario Lagoas-Marcosende, University of Vigo, 36310 Vigo, Spain
[b]Área de Mecánica de Fluidos, Escuela de Ingeniería Industrial, Campus Universitario Lagoas-Marcosende, University of Vigo, 36310 Vigo, Spain
* Author for correspondence: E-mail: jsieres@uvigo.es, Tel: +34 986 811997, Fax: +34 986 811995

ABSTRACT

This paper is focused on a small power refrigeration cycle demonstration unit to be used at different operating conditions and in various fields of study. The refrigeration unit is planned to be used principally for two different kinds of studies: thermodynamic analyses of the refrigeration system performance at different evaporation and condensation temperatures; and determination of the heat transfer coefficients during the condensation and evaporation processes.

In order to design and select its different components, a detailed simulation model was developed. The model takes into account specific data, characteristics and dimensions of the main components.

In the paper, the main components of the refrigeration unit are described, the mathematical simulation model is detailed and the main results of the simulation model are presented and analyzed.

NOMENCLATURE

Cp	[J/(kg K)]	Specific heat capacity
d	[m]	Diameter
DS	[K]	Degree of superheat
f	[Hz]	Frequency
h	[J/kg]	Specific enthalpy
k	[W/(m K)]	Thermal conductivity
L	[m]	Length
m	[kg/s]	Mass flow rate
N	[rad/s]	Speed regime
N_s	[rad/s]	Synchronous speed
p	[kPa]	Pressure
p_m	[-]	Number of magnetic pole pairs per phase
q	[W]	Heat flow
q"	[W/m^2]	Heat flux
R	[K/W]	Thermal resistance
RC		Pressure ratio
R^2		Coefficient of determination
s_m	[-]	Slip
T	[K], [ºC]	Temperature
V	[m^3/s]	Volumetric flow rate
V_t	[m^3]	Compressor displacement
W	[W]	Power

Greek symbols

α	[W/(m^2 K)]	Heat transfer coefficient
ΔT_{lm}	[K]	Logarithmic mean temperature difference
ρ	[kg/m^3]	Density
η	[-]	Efficiency

Subscripts

ac	Air-cooled heat exchanger
air	Air
cl	Convective liquid flow
C	Condenser
e	External
E	Evaporator
elec	Electric
i	Internal
in	Inlet
is	Isentropic
n	Nucleate pool boiling
out	Outlet
ov	Overall
sat	Saturation conditions
t	Tube wall
ref	Refrigerant
Vol	Volumetric
w	Water

INTRODUCTION

Air-conditioning and refrigeration installations account for about 30 percent of worldwide energy consumption [1]. Thus deep knowledge of this type of installations is of great importance in the actual energy and industrial scenario. Even though, there are different refrigeration technologies in the market, the most extended one is the vapor compression technology.

As a result, most engineering courses all over the world cover, in more or less depth, fundamental and advanced topics related with vapor compression systems. Usually the preferred method of teaching technological disciplines is an alternation between traditional classrooms, in which the teacher introduces the contents of the subject matter or solves exercises, and other activities such as the use of multimedia files, web-based applications, simulation software and experimental equipment. In the field of refrigeration a broad number of examples exist, such as those found in Refs. [2-5].

A number of experimental equipment for lecture in vapor compression refrigeration systems exist in the market. However, this type of equipment is usually either expensive or limited to a set of experiments focused on the demonstration principles of the technology rather than on the possibility of carrying out detailed and controlled thermodynamic or heat transfer analyses.

This paper is focused on a small power refrigeration demonstration unit based in the vapor compression cycle. The refrigeration unit is planned to be used principally for two different kinds of studies: thermodynamic analyses of the refrigeration system performance at different evaporation and condensation temperatures; and determination of the heat transfer coefficients during the condensation and evaporation processes.

The design and selection of its components are focused to meet the following challenges:

1. The user should be able to perform basic thermodynamic analyses; as a result, the experimental unit has to be equipped with proper instrumentation.

2. The user should be able to perform (and repeat) experimental tests at the desired operating conditions (basically condensation and evaporation temperatures); thus, the experimental unit has to be equipped with adequate operational or electronic control systems.

3. The user should be able to calculate the condensation and evaporation heat transfer coefficients. This requires that the instrumentation used and the operating conditions found in the condenser and evaporator should be studied in detailed in order to be favorable for measuring the heat transfer coefficients with a reasonable accuracy.

In order to design and select its different components, a detailed simulation model was developed. The model takes into account specific data, characteristics and dimensions of the main components. In the paper, the main components of the refrigeration unit are described, the mathematical simulation model is detailed and the main results of the simulation model are presented and analyzed.

DESCRIPTION OF THE DEMONSTRATION UNIT

The mathematical simulation is based on an experimental demonstration unit which operating scheme is depicted in Figure 1. The demonstration unit consists of the main components found in a vapor compression refrigeration unit: compressor, condenser, expansion device and evaporator. The compressor and expansion device are commercially available but the heat exchangers (condenser and evaporator) have been specially design to perform different heat transfer analyses. The refrigerant used is R134a.

The evaporator consists of a vertical copper tube of diameter 9.52/7.92 mm and 1 m length. The evaporator is covered by a flexible power heating cable that supplies a uniform heating power along the evaporator length. The total heating power supplied to the evaporator (equal to the evaporator cooling capacity) is adjusted modifying the heating cable supply voltage by means of a rheostat. The refrigerant flows vertically from the bottom to the top of the evaporator. The refrigerant enters the evaporator as a two-phase flow and leaves it as a superheated vapor flow. The degree of superheat at the evaporator outlet is controlled manually by a commercial thermostatic expansion valve.

The condenser consists of two concentric copper tubes of 1 m length which are oriented vertically. The inner and outer tubes are of diameters 15.87/14.13 mm and 9.52/7.92 mm, respectively. The refrigerant condensation takes place as it flows downwards inside the inner tube. Water is used as the cooling medium which flows through the annular space formed by the concentric tubes, in counter current with the refrigerant flow.

The cooling water flows in a closed loop consisting of a circulating pump and a forced air-cooled heat exchanger, constructed with copper tube of 3/8" in staggered arrangement and continuous aluminum fins. The cooling water temperature can be adjusted by controlling the airflow of the fan of the air-cooled heat exchanger by means of a variable frequency drive.

The compressor is a commercial hermetic compressor with a displacement of 3.13 cm^3. The refrigerant mass flow rate is controlled by varying the compressor supply frequency by means of a variable frequency drive.

Other components of the experimental demonstration unit are a thermostatic expansion valve, solenoid valve, filter and proper instrumentation, as depicted in Figure 1.

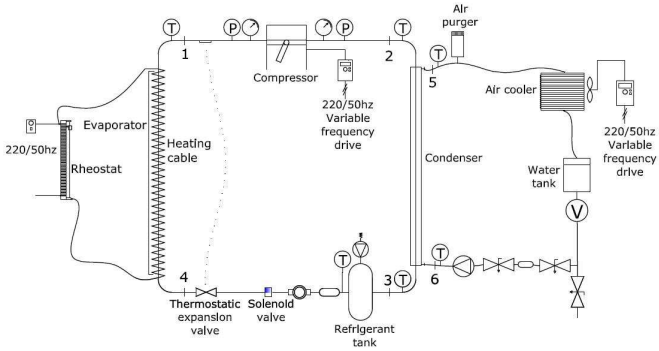

Figure 1 Schematic representation of the experimental demonstration unit.

SYSTEM MODELLING

A steady state mathematical model has been developed in order to simulate the vapor compression demonstration unit. The model takes into account specific data and dimensions of the components in order to predict the real operating conditions of the unit. The following general assumptions have been considered:

1. The system operates at steady-state conditions.

2. The pressure drops in the refrigerant pipes circuit are negligible.

3. Heat transfer between the heat exchangers and the surroundings is negligible

4. The heat losses from the refrigerant and water lines are negligible.

5. Saturated liquid conditions are considered at the outlet of the condenser.

6. In order to obtain the thermodynamic state at the compressor outlet, the compression process is considered to be

isentropic. Later, the overall compressor efficiency is used to calculate the electric power of the compressor.

In the following sections the basic characteristics and equations of the main components of the experimental unit are detailed.

Compressor

The Danfoss TL3G hermetic compressor was selected with a displacement of 3.13 cm^3. The refrigerant used is R134a. The manufacturer reports data for the capacity and power consumption of the compressor for a condensing temperature of 55 ºC and an evaporating temperature range of -30 to 15 ºC, measured according to the test conditions of EN 12900/CECOMAF and ASHRAE standards.

The pressure ratio of the compressor is defined as the ratio of the discharge pressure to suction pressure. According to assumption 2, these pressures are the condensation and evaporation pressures, respectively. Then, the pressure ratio is given by equation (1):

$$RC = \frac{p_C}{p_E} \tag{1}$$

The refrigerant mass flow rate can be obtained from the compressor displacement (V_t), speed regime (N), volumetric efficiency (η_{Vol}) and the refrigerant density at the suction conditions (ρ_1), as stated in equation (2):

$$m_{ref} = \rho_1 \cdot V_t \cdot \eta_{vol} \cdot N / (2 \cdot \pi) \tag{2}$$

The manufacturer reports data for different operating conditions and supply frequencies of 50 and 60 Hz. The compressor speed (N) is related to the supply frequency by equations (3) and (4):

$$N_s = \frac{2 \cdot \pi \cdot f}{p_m} \tag{3}$$

$$s_m = \frac{N_s - N}{N_s} \tag{4}$$

where N_s is the synchronous speed, f is the supply frequency, p_m is the number of magnetic pole pairs per phase and s is the slip. In our case $p_m = 1$ and a typical value of $s_m = 5\%$ for small motors has been assumed.

The volumetric efficiency was obtained by a simple regression analysis from the refrigeration data capacity provided in the manufacturer technical data. Figure 2 shows the values of the volumetric efficiency as a function of the pressure ratio. It can be seen that a linear dependence exists between the experimental values of the volumetric efficiency and the pressure ratio, and also that this dependency is not affected by the compressor supply frequency (50 or 60 Hz). Equation (5) is the result of the regression analysis with a coefficient of determination R^2 higher than 99%.

$$\eta_{vol} = -0.02372 \cdot RC + 0.7396 \tag{5}$$

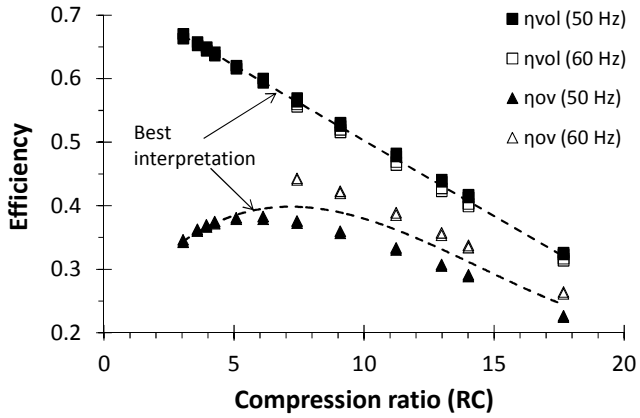

Figure 2 Volumetric efficiency and overall efficiency of the compressor as a function of the pressure ratio.

The isentropic power of the compressor (W_{is}) can be calculated as stated in equation (6):

$$W_{is} = m_{ref} \cdot (h_{2is} - h_1) \tag{6}$$

where h_{2is} is the specific enthalpy of the refrigerant vapor at the discharge pressure and specific entropy of the refrigerant vapor entering the compressor.

The overall efficiency of the compressor is obtained as the ratio of the isentropic power to the real power consumption obtained from the manufacturer data:

$$\eta_{ov} = \frac{W_{is}}{W_{elec}} \tag{7}$$

Only the compressor power consumption is given by the manufacturer, so only the overall efficiency could be determined and other compressor efficiencies such as the indicated or electrical efficiency could not be calculated.

Figure 2 also shows the values of the compressor overall efficiency as a function of the pressure ratio obtained from the manufacturer data. With respect to the results of the volumetric efficiency, two main differences are observed. The first one is that a linear dependence between the overall efficiency and the pressure ratio cannot be assumed, so a higher order polynomial fit should be considered. The second difference is that the overall efficiency is affected by the compressor supply frequency (50 or 60 Hz). Anyway, due to the information is only limited to two frequency values (50 and 60 Hz), the effect of the frequency was neglected and the overall efficiency was assumed to be only a function of the pressure ratio. Eq. (8) is the result of the regression analysis with a coefficient of determination R^2 of 80%.

$$\eta_{ov} = 1.24 \cdot 10^{-4} \cdot RC^3 - 5.37 \cdot 10^{-3} \cdot RC^2 + 0.05786 \cdot RC + 0.2139 \tag{8}$$

Thermostatic valve

The thermostatic valve is assumed to be perfectly isolated, so the refrigerant suffers an isenthalpic process ($h_3 = h_4$). The

thermostatic valve guarantees a constant degree of superheat at the evaporator outlet, then:

$$T_1 = T_{sat}(p_E) + DS \quad (9)$$

where T_{sat} represents the saturation temperature at the evaporator pressure and DS is the constant degree of superheat controlled by the thermostatic valve.

Condenser

The condenser consists of two concentric copper tubes oriented vertically of 1 m length. The heat transfer rate from the refrigerant to the cooling medium (water) can be obtained by applying energy balances for each stream – equations (10) and (11) – and the heat transfer equation (12).

$$q_C = m_{ref} \cdot (h_2 - h_3) \quad (10)$$

$$q_C = m_w \cdot Cp_w \cdot (T_5 - T_6) \quad (11)$$

$$q_C = \frac{\Delta T_{lm,C}}{R_C} \quad (12)$$

where $\Delta T_{lm,C}$ is the logarithmic mean temperature difference and R_C is the overall thermal resistance in the condenser:

$$R_C = R_{iC} + R_{tC} + R_{eC} = \frac{1}{\alpha_{iC} \cdot \pi \cdot d_{iC} \cdot L_C} + \frac{\ln(d_{eC}/d_{iC})}{2 \cdot \pi \cdot k_t \cdot L_C} + \frac{1}{\alpha_{eC} \cdot \pi \cdot d_{eC} \cdot L_C} \quad (13)$$

The condensation process takes place inside the inner tube of the condenser, so it is affected by the vapor flow which also flows downwards. The liquid film is then expected to be thinner than in the absence of vapor flow, so a higher condensation heat transfer coefficient should be expected. In this work, the average heat transfer coefficient (α_{iC}) has been obtained from McNaught and Butterworth [6].

The heat transfer coefficient (α_{eC}) for turbulent flow in the concentric annular duct was calculated according to Petukhov and Roizen [7], using a modified form of the Gnielinski [8] correlation for turbulent flow in tubes as a function of the inner and outer tubes diameters ratio.

Evaporator

The evaporator consists of a vertical copper tube of 1 m length. A uniform heating power (q_E) along the evaporator length is supplied by means of a flexible power heating cable. The heat transfer rate can be related with the refrigerant conditions by applying the energy balance for the refrigerant flow, as stated in equation (14).

$$q_E = m_{ref} \cdot (h_1 - h_4) \quad (14)$$

The boiling heat transfer process inside the vertical tube of the evaporator is modeled by the additive formula recommended by Rohsenow and Griffith [9]:

$$q''_E = q''_n + q''_c \quad (15)$$

In this expression, q''_n is the nucleate pool boiling heat flux calculated from Rohsenow [10] based on the assumption that the bulk of the liquid is stationary. The term q''_c is the single-phase convective heat flux obtained from equation (16):

$$q''_c = \alpha_{cl} \cdot (T_{tE} - T_E) \quad (16)$$

where α_{cl} is calculated from the Dittus-Boelter correlation [11] based on the assumption that a single-phase liquid flow at temperature T_E flows inside the tube. Rohsenow and Griffith [9] recommend calculating α_{cl} by replacing the coefficient 0.023 with 0.019 in the Dittus-Boelter correlation.

Refrigeration system

The system COP is obtained from equation (17):

$$COP = \frac{q_E}{W_{elec}} \quad (17)$$

In this equation, the refrigeration capacity is calculated as stated in equation (14) and the electric power consumption of the compressor is calculated using equations (6) to (8).

Cooling water pump

The Wilo Star-RS 25/7 circulation pump is used for the cooling water circuit. The total head (kPa) for different water flow rate values (m^3/s) was obtained from the manufacturer technical data. These values were fitted by a simple regression analysis which result yields equation (18) with a coefficient of determination R^2 higher than 99%.

$$\Delta p = -1.468 \cdot 10^7 \cdot V_w^2 - 1.4272 \cdot 10^4 \cdot V_w + 65.57 \quad (18)$$

Air-cooled heat exchanger

The forced air-cooled heat exchanger has a heat transfer area of 1 m^2 and it is constructed with eight copper tubes of 9.5/7.9 mm in staggered arrangement and continuous aluminum fins. The configuration is of a single-pass, cross-flow heat exchanger with both fluids unmixed.

The heat transfer rate is estimated based on manufacturer data (EN-327:2000) by equation (19).

$$q_{ac} = q_C = q_{15} \cdot \frac{\Delta T_{lm,ac}}{15} \quad (19)$$

where $\Delta T_{lm,ac}$ is the logarithmic mean temperature difference between the water and air flows, and q_{15} is the heat transfer rate for a temperature difference of 15 K. Equation (19) is based on performance data for an air cooled refrigerant condenser and not an air cooled water flow heat exchanger. However, equation (19) was considered to be valid (or at least conservative) based on the following considerations: a quick evaluation of the overall heat transfer coefficient indicated that the air side thermal resistance was the higher one; the water flow rate is very high, so the water side temperature is nearly constant; and, the water side flow regime is turbulent, so high water side heat transfer coefficients are obtained.

An energy balance on the air side gives equation (20):

$$q_{ac} = V_{air} \cdot \rho_{air} \cdot Cp_{air} \cdot \left(T_{air,out} - T_{air,in}\right) \quad (20)$$

where V_{air} is the nominal air flow rate.

Cooling water circuit

A total tube length of 2 m of copper tube of diameter 15.9/14.1 mm is considered for the cooling water circuit, excluding the condenser length and the tube-side length of the air-cooled heat exchanger. The pressure drops in the connecting tubes as well as the pressure losses in the piping components, air-cooled heat exchanger and flow-meter were considered in conjunction with the pump curve to determine the water flow rate [12].

RESULTS AND DISCUSSION

The mathematical model described in the previous section has been programmed using Engineering Equation Solver (EES) [13]. The model has been used to simulate and analyze the performance of the experimental vapor compression demonstration unit under different operating conditions. The input parameters and operating conditions considered for the analysis are indicated in Table 1.

Table 1. Operating conditions and components data.

Parameters	Values
Compressor	
Displacement	$3.13 \cdot 10^{-6}$ m^3
Number of magnetic pole pairs per phase	1
Number of phases	1
Slip	5%
Supply frequency	50 Hz
Volumetric efficiency	Eq. (5)
Overall efficiency	Eq. (8)
Condenser	
Length	1 m
Tube material	Copper
Inner tube diameters	15.9/14.1 mm
Outer tube diameters	9.5/7.9 mm
Condensation temperature	50 ºC
Evaporator	
Length	1 m
Tube material	Copper
Tube diameters	9.5/7.9 mm
Evaporation temperature	5 ºC
Thermostatic valve	
Degree of superheat	5 K
Water pump	
Pump curve	Eq. (18)
Air-cooled heat exchanger	
Nominal temperature difference	15 K
Nominal heat transfer rate (q_{15})	450 W
Nominal air flow rate	0.115 m^3/s
Number of tubes	8
Tubes length	0.262 m
Tube material	Copper
Tubes diameters	9.5/7.9 mm

Thermodynamic analysis

Table 2 shows the numerical results of the simulation model, considering the data in Table 1. It can be seen, that for the given data, the system COP is 1.72. The maximum ambient temperature of 29.4 ºC indicates that if the ambient temperature is higher than this value then it would not be possible to carry out this experiment (for the given values of condensation and evaporation temperatures). In contrast, if the ambient temperature is lower than the calculated value, then the experiment can be easily attained if the speed of the fan of the air-cooled heat exchanger is adjusted to the required value by means of the variable frequency drive. Similarly, in order to operate at the input evaporation temperature, the heating cable supply voltage should be adjusted by means of the rheostat in order to obtain the heating power value (equal to the cooling power) shown in Table 2.

Table 2. Calculated parameters of the experimental demonstration unit

Parameters	Values
Vapor compression system	
Evaporation pressure	350 kPa
Condensation pressure	1320 kPa
Refrigerant mass flow rate	$1.61\ 10^{-3}$ kg/s
Cooling power	217 W
Condensation heat power	263 W
Compressor isentropic power	46 W
Compressor electric power	126 W
COP	1.72
Cooling water circuit	
Water flow rate	$3.34 \cdot 10^{-4}$ m^3/s
Inlet water temperature to condenser (T_6)	39.0 ºC
Outlet water temperature from condenser (T_5)	39.2 ºC
Air-cooled heat exchanger	
Maximum required ambient temperature ($T_{air,in}$)	29.4 ºC
Logarithmic mean temperature difference	8.8 ºC

It is known that for a vapor compression system, the COP increases with increasing values of the evaporation temperature and decreasing values of the condensation temperature. Figure 3 shows the numerical results predicted by the simulation model for condensation and evaporation temperature values in the range from 35 to 60 ºC and from 0 to 15 ºC, respectively.

Figure 4 shows the results for the pressure ratio for the same cases analyzed in Figure 3. It can be seen that the pressure ratio increases with increasing values of the condensation temperature and with decreasing values of the evaporation temperature. As a result, an opposed trend should be expected for the compressor volumetric efficiency, which is confirmed in the numerical results shown in Figure 5. Figure 5 also shows the results for the overall compressor efficiency. For the range of condensation and evaporation temperature values analyzed, the pressure ratio is always lower than 6; then, from equation (8) and figure 2, it should be expected that the overall compressor efficiency increases with increasing values of the condensation temperature and with decreasing values of the evaporation temperature, as confirmed in Figure 5.

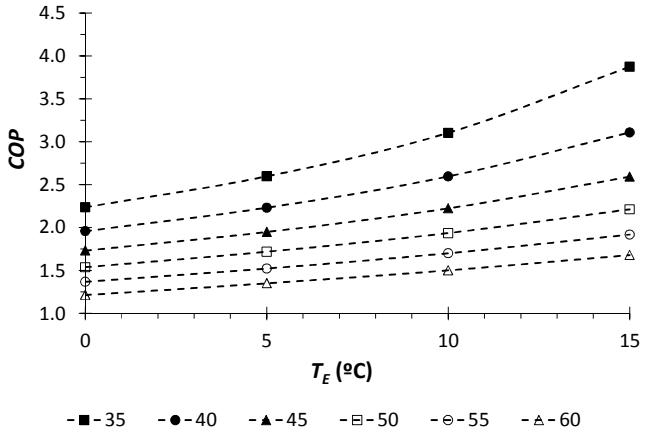

Figure 3 System COP as a function of the evaporation temperature for different values of the condensation temperature.

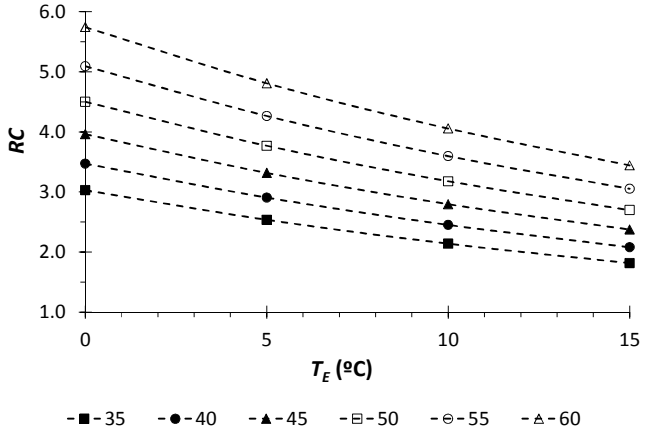

Figure 4 Pressure ratio (*RC*) as a function of the evaporation temperature for different values of the condensation temperature.

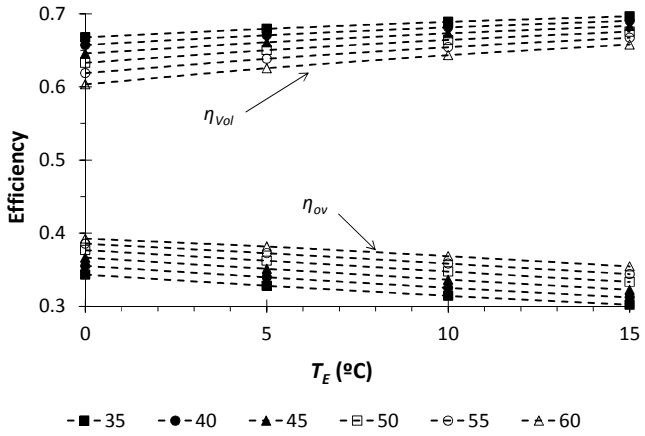

Figure 5 Volumetric and overall compressor efficiencies as a function of the evaporation temperature for different values of the condensation temperature.

The range of evaporation and condensation temperature values that would be possible to test with the refrigeration cycle demonstration unit will be constrained by the ambient air temperature. Figure 6 shows the calculated ambient temperature values ($T_{air,in(\max)}$) required to perform these experimental tests. If the actual ambient temperature is lower than the values shown in figure 6, then the experiment can be attained reducing the speed of the fan of the air-cooled heat exchanger by means of the variable frequency drive. In contrast, if the ambient temperature is higher than the values calculated in figure 6, then it would not be possible to perform the experiment with the corresponding evaporation and condensation temperature values. Results shown in figure 6 indicate that $T_{air,in(\max)}$ decreases with the decreasing values of the condensation temperature and with increasing values of the evaporation temperature. This last behavior is expected, since when the evaporation temperature is increased for a fixed value of the condensation temperature, then the compression ratio decreases and, according to figure 4, the volumetric efficiency increases. As a result, higher values of the refrigerant mass flow rate and higher values of the cooling and condensation powers are obtained.

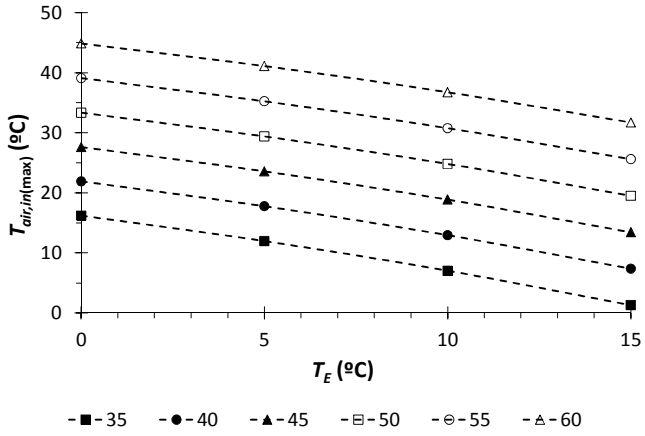

Figure 6 Maximum required ambient temperature as a function of the evaporation and condensation temperatures.

Heat transfer analysis

The refrigeration cycle demonstration unit is also planned to be used for the determination of the heat transfer coefficients during the condensation and evaporation processes.

In a first stage, the condensation heat transfer coefficient will be studied for different pure refrigerants and refrigerant mixtures. Since only fluid temperatures are measured (wall temperatures are not measured) a tentative technique for determining the condensation heat transfer coefficient will be the use of the Wilson plot method [14] or some of its modifications [15]. In order to apply the Wilson plot method successfully, at least the following conditions are desirable: a) the temperature difference between the condensing refrigerant and the water stream is high enough to be only gently affected by the accuracy of the temperature sensors; b) the main thermal resistance in the condenser is the condensation side thermal resistance; and, c) during different experimental tests the wall

conductive and water convective thermal resistance remain nearly constant when compared with the overall thermal resistance variation.

Figure 7 shows the results for the logarithmic mean temperature difference in the condenser ($\Delta T_{lm,C}$). It can be seen that for all the operating conditions considered, $\Delta T_{lm,C}$ is always higher than 8 ºC, which will be easily measured (with sufficient accuracy) in the future experiments.

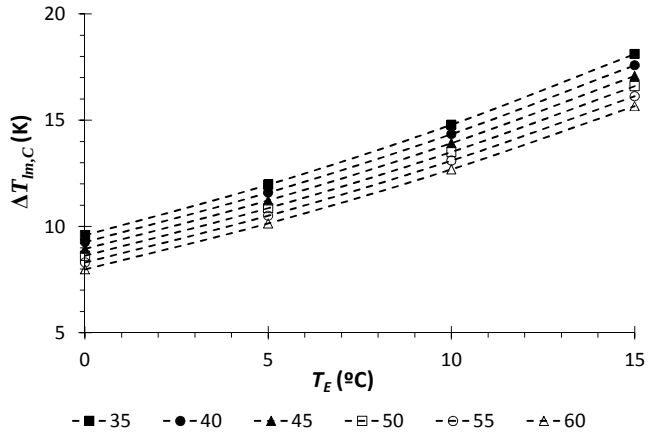

Figure 7 Logarithmic mean temperature difference in the condenser as a function of the evaporation and condensation temperatures.

The results of the thermal resistances in the condenser are collected in Figure 8. It can be seen that the overall thermal resistance in the condenser (R_C) increases with the evaporation and condensation temperatures. For all the cases analyzed, results in Figure 8 show that the thermal resistance of the condensation process accounts for more than 90% of the overall thermal resistance in the condenser.

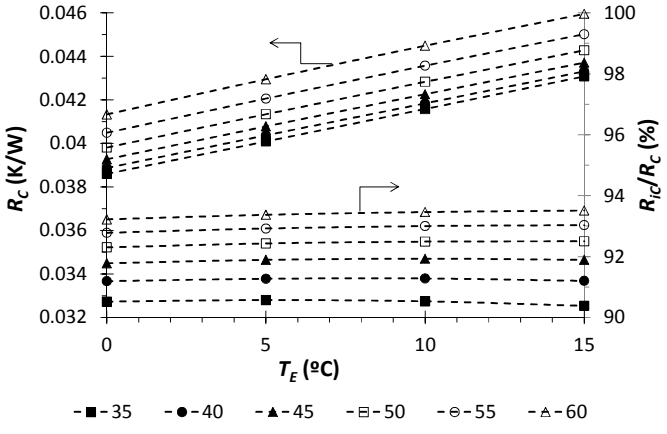

Figure 8 R_C and ratio R_{iC}/R_C as a function of the evaporation and condensation temperatures.

All previous results rely on the assumption that the heat transfer coefficients can be determined or estimated from published correlations. However, typical accuracies of these correlations can be as high as 30%. Therefore a sensitivity analysis of the effect of the heat transfer coefficients on the overall thermal resistance has been performed. The results of this analysis are shown in Figure 9. The water heat transfer coefficient, the condensation heat transfer coefficient and the tube wall thermal conductivity have been multiplied by a factor varied from 0.1 to 10. It can be seen that the condensation heat transfer coefficient (α_{iC}) has the most significant effect on the overall thermal resistance (R_C). The water side heat transfer coefficient (α_{eC}) is the next more important factor, though its effect is much lower. Finally, the tube wall thermal resistance is negligible. These results show that the experimental unit design and operating conditions are adequate to experimentally measure the condensation heat transfer coefficient even if the water side heat transfer coefficient calculation cannot be estimated with accuracies better than 30%.

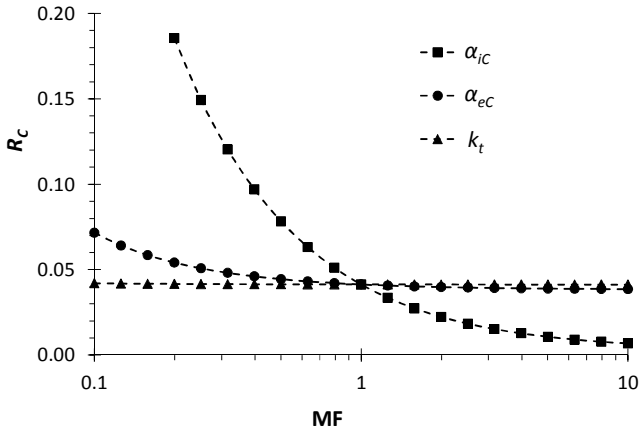

Figure 9 Effect of the heat transfer coefficients on the condenser thermal resistance.

CONCLUSIONS

This paper covered the design and simulation of a small power refrigeration cycle demonstration unit to be used at different operating conditions and in various fields of study. In order to predict the performance of the refrigeration unit, the simulation model accounted for specific data, characteristics and dimensions of the main components.

The results of the simulation model indicated that the refrigeration unit will be able to be used for two different kinds of studies: thermodynamic analyses of the refrigeration system performance at different evaporation and condensation temperatures; and determination of the heat transfer coefficients during the condensation and evaporation processes.

The evaporation temperature will be experimentally controlled by adjusting the total heating power supplied to the evaporator by means of a rheostat that varies the heating cable supply voltage. On the other hand, the condensation temperature will be controlled by varying the airflow of the fan of the air-cooled heat exchanger by means of a variable frequency drive. However, it was shown that for some combinations of the evaporation and condensation temperatures, it may not be possible to carry out the experiment because it would require too low ambient air temperatures.

ACKNOWLEDGMENTS

The authors would like to acknowledge the financial support from the "Xunta de Galicia", Project 09REM004303PR.

REFERENCES

[1] Buzelin L.O.S, Amico S.C., Vargas J.V.C., Parise J.A.R., Experimental development of an intelligent refrigeration system, *Int. J. Refrigeration*, Vol. 28, 2005, pp. 165–175.

[2] Sieres J., Fernández-Seara, J., Simulation of compression refrigeration systems, *Comput. Appl. Eng. Educ.*, Vol. 14, 2006, pp. 188–197.

[3] CoolPack 1.49:
http://www.ipu.dk/English/IPU-Manufacturing/Refrigeration-and-energy-technology/Downloads/CoolPack.aspx

[4] Tan F.-L., Ameen A., Fok S.-C., Engineering courseware on refrigeration cycle simulation, *Comput. Appl. Eng. Educ.*, Vol. 5, 1997, pp. 115–120

[5] Abu-Mulaweh H. I., Computer-controlled air-conditioning experimental apparatus, *Comput. Appl. Eng. Educ.*, Vol. 18, 2010, pp. 458–468

[6] McNaught J.M., Butterworth D., Film condensation of pure vapour, in: Hewitt G.F. (Ed.), *Heat Exchanger Design Handbook*, Begell House, New York, 1998, 2.6.2.

[7] Petukhov B.S. Roizen L.I., Generalized relationship for heat transfer in a turbulent flow of a gas in tubes of annular section, *High Temp. (URSS)*, Vol. 2, 1964, pp. 65-68.

[8] Gnielinski V., New equations for heat and mass transfer in turbulent pip and channel flow, *Int. Chem. Eng.*, Vol. 16, 1976, pp. 359-368.

[9] Rohsenow W.M. Griffith P., Correlation of maximum heat flux data for boiling of saturated liquids, *AIChE-ASME Heat Transfer Symp.*, Louisville, Ky., 1955.

[10] Rohsenow W.M., A method of correlating heat transfer data for surface boiling liquids, *Trans. ASME*, Vol. 74, 1952.

[11] Dittus PW. And Boelter L.M.K., Heat transfer in automobile radiators of the tubular type, *Int. Commun. Heat Mass Transfer*, Vol. 12, 1985, pp. 3-22.

[12] Gersten K., Ducts, in: Hewitt G.F. (Ed.), *Heat Exchanger Design Handbook*, Begell House, New York, 1998, 2.2.2.

[13] Klein S.A., Engineering Equation Solver (EES), F-Chart Software, Middleton, WI, 1992-2006.

[14] Wilson E.E., A basis for rational design of heat transfer apparatus, *Trans. ASME*, Vol. 37, 1915, pp. 47–82.

[15] Fernández-Seara J., Uhía F.J., Sieres J., Campo A., A general review of the Wilson plot method and its modifications to determine convection coefficients in heat exchange devices, *Appl. Therm. Eng.*, Vol. 27, 2007, pp. 2745-2757.